Temperature and Solvent Dependence of Stiffness of Poly{*n*-hexyl-[(*S*)-3-methylpentyl]silylene} in Dilute Solutions

Ken Terao,[†,⊥,∥] Yoshimi Terao,[†,⊥] Akio Teramoto,*[†,⊥] Naotake Nakamura,[†,⊥] Michiya Fujiki,[‡,⊥] and Takahiro Sato[§,⊥]

Research Organization of Science and Engineering, Ritsumeikan University, 1-1-1 Nojihigashi, Kusatsu, Siga 525-8577, Japan; NTT Basic Research Laboratories, 3-1 Wakamiya, Morinosato, Atsugi, Kanagawa 243-0198, Japan; Department of Macromolecular Science, Osaka University, Machikaneyama-cho 1-1, Toyonaka, Osaka 560-0043, Japan; and CREST-JST (Japan Science and Technology Corporation), 4-1-8 Honcho, Kawaguchi, Saitama 332-0012, Japan

Received February 5, 2001

ABSTRACT: Eleven samples of poly{*n*-hexyl-[(*S*)-3-methylpentyl]silylene} (PH3MPS) ranging in weight-average molecular weight M_w from 3.1×10^3 to 8.7×10^5 in isooctane have been studied by light scattering at 25 °C, sedimentation equilibrium at 25 °C, and viscometry at five temperatures (−27,−15, 5, 25, and 45 °C) to determine their *z*-average radii of gyration $\langle S^2 \rangle_z$, second virial coefficients, and intrinsic viscosities $[\eta]$. The $\langle S^2 \rangle_z$ and $[\eta]$ data are analyzed quantitatively by the current theories on the basis of the wormlike chain with excluded volume over the entire range of M_w studied. PH3MPS is shown to be a typical semiflexible polymer with the persistence length changing from 15.4 to 5.0 nm at −27 to 45 °C. The viscometry has also been made on a PH3MPS sample in *n*-hexane and methylcyclohexane at 25 °C. In these solvents, the global conformation of PH3MPS is essentially the same as that in isooctane at the same temperature.

Introduction

Polysilylenes, whose main chains consist of Si−Si bonds, have a particular nature, that their conformations are closely correlated with their electronic structures. Indeed, it has been found that their UV spectra, optical activities, etc., change sensitively with the chemical structure of side chains and solvent conditions, which in turn determine the backbone conformation.[1−3]

In 1990s, Fujiki et al. synthesized a variety of polysilylenes, which have dialkyl or aryl−alkyl side chains with or without chiral carbons.[4−14] They measured Mark−Houwink−Sakurada (MHS) exponents α and UV absorption spectra and showed that the global conformations as detected by viscosity of these polymers are closely correlated with the peak height and the half-peak-height width of height of their UV spectra.[7] This study is an important step toward exploiting the universal correlation between the backbone conformation and the electronic structure of polysilylenes.

However, these data may not be used for quantitative discussions because the MHS equation is correct only over a limited molecular weight range.[15,16] In this connection, it has been shown that dimensional and hydrodynamic properties of unperturbed polymer chains, either flexible or stiff, are explained almost quantitatively on the basis of the Kratky−Porod wormlike chain[17] or Yamakawa's more general model called the helical wormlike chain.[15] The persistence length *q*, a parameter of this model, is a better measure for stiffness than the viscosity exponents.

Cotts[18] analyzed dimensional and hydrodynamic data for poly(di-*n*-hexylsilylene) at the Θ state, using a mixed Θ solvent, on the basis of the unperturbed wormlike chain, to find that the *q* value was 3.5 nm. However, as far as we know, this is the only *q* value reported for polysilylenes. It is necessary to study a large number of polysilylenes with different side chains in order to elucidate the correlation between the global conformation and electronic structure of these polymers.

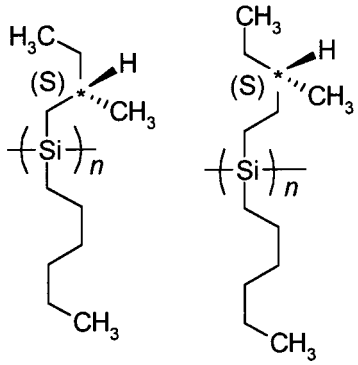

1 **2**

Figure 1. Chemical structures of PH2MBS (**1**) and PH3MPS (**2**).

Very recently, we made a light scattering and viscosity study of two chiro-optical polysilylenes[19] whose chemical structures are shown in Figure 1: poly{*n*-hexyl[(*S*)-2-methylbutyl}silylene] (PH2MBS) and poly-[*n*-hexyl-{(*S*)-3-methylpentyl}silylene] (PH3MPS). It was found that the persistence length in isooctane is 85 nm for PH2MBS at 20 °C and 6.1 nm for PH3MPS at 25 °C; namely, the former is almost rodlike, whereas the latter is semiflexible. In the present study we have expanded this viscosity study of PH3MPS in isooctane at temperatures other than 25 °C between −27 and 45 °C, in *n*-hexane at 25 °C, and in methylcyclohexane at 25 °C. In this paper, we present the experimental details including sample preparation and light scattering,

† Ritsumeikan University.
‡ NTT Basic Research Laboratories.
§ Osaka University.
⊥ CREST-JST.
∥ Present address: Department of Biological and Chemical Engineering, Faculty of Engineering, Gunma University, Kiryu, Gunma 376-8515, Japan.

10.1021/ma010212w CCC: $20.00 © 2001 American Chemical Society
Published on Web 05/25/2001

which has not been described in our previous paper.[19] Then the data for intrinsic viscosities and scattering radii obtained are analyzed by the current theories[15,20,21] for wormlike chain with or without excluded volume.

Experimental Section

Samples. A PH3MPS sample was obtained by a sodium-mediated condensation of dichloro-*n*-hexyl-[(*S*)-3-methylpentyl]-silane in hot toluene with 18-crown-6. This PH3MPS sample dissolved in a mixed solvent (toluene 90% + cyclohexane 10%) was separated into seven fractions (F1, F2, ..., F7) and an oligomer fraction on a Shodex 2006M column (20 mm i.d. and 300 mm long) in about 500 runs. In each run a 1 cm^3 solution with the mass concentration 5×10^{-3} g cm^{-3} was fed on the machine and eluted at a flow rate of 2.5 cm^3/min. Each fraction except for the oligomer fraction was separated into three fractions on the same column, the middle fractions (F12, F22, ..., F72) were chosen for this study, and the third fraction of F4 (F43) and the first fraction of F6 (F61) were used to study solvent effects. The oligomer fraction was separated into four fractions (O1, O2, O3, and O4) on a Shodex 2003 column (the same size as 2006M). These fractions were also used for physical measurements.

PH3MPS samples are photodegradable, and the specific viscosity of their dilute solutions sharply decreased by illuminating natural light. Therefore, the sample preparation mentioned above and physical measurements described below were made by shielding room light as much as possible. It was confirmed by viscosity that molecular weight of the samples did not change while studied.

The polydispersity of each sample was estimated by gel permeation chromatography (GPC) with a detector operating at 320 nm under the following conditions: two columns of Shodex 806M, connected in series, tetrahydrofuran at 40 °C as the eluent, and flow rate of 1 cm^3 min^{-1}.

Sedimentation Equilibrium. Values of the weight-average molecular weight M_w and the second virial coefficient A_2 for PH3MPS samples of O1, O2, O3, and O4 in isooctane at 25 °C were determined by sedimentation equilibrium on a Beckman Optima XL-1 analytical ultracentrifuge. Aluminum 12 mm double-sector cells were used. The height of the solution column was adjusted to 1.5 mm, and the rotor speed was chosen so that the equilibrium polymer concentration c_b at the cell bottom is about 3 times the concentration c_a at the meniscus. These concentrations were detected by an interferential optics operating at 675 nm.

The data obtained were analyzed according to the equation

$$M_{app}^{-1} = M_w^{-1} + 2A_2\,\bar{c} \tag{1}$$

where the apparent molecular weight M_{app} and the mean concentration $\bar{c}$ are defined by

$$M_{app} = (c_b - c_a)/\lambda c_0 \tag{2}$$

$$\bar{c} = (c_b + c_a)/2 \tag{3}$$

with

$$\lambda = (r_b^2 - r_a^2)(1 - \bar{\nu}\rho_0)\omega^2/2RT \tag{4}$$

In these equations, r_a and r_b are the radial distances from the center of rotation to the meniscus and the cell bottom, respectively, $\bar{\nu}$ is the partial specific volume of the polymer, ρ_0 is the solvent density, ω is the angular velocity of the rotor, R is the gas constant, and T is the absolute temperature.

Ratios of M_z (the z-average molecular weight) to M_w were estimated from the sedimentation equilibrium data by use of the equation

$$Q = (M_w/M_z)(1 + 2A_2M_w\bar{c} + ...) \tag{5}$$

where

$$Q = \frac{(c_b - c_a)^2}{c_0(r_b^2 - r_a^2)[(\partial c/\partial r^2)_{r=r_b} - (\partial c/\partial r^2)_{r=r_a}]} \tag{6}$$

The specific refractive index increments $\partial n/\partial c$ of PH3MPS in isooctane at 25 °C were determined using an OPTILAB DSP interferometic refractometer for 633 nm wavelength and a modified Schulz-Cantow type differential refractometer for 436 and 546 nm. The result at 436, 546, and 633 nm were 0.192, 0.172, and 0.162 cm^3 g^{-1}, respectively; note that molecular weight dependence of $\partial n/\partial c$ was negligible (less than 1.2%) even for the sample of lowest molecular weight studied here. The plot of $\partial n/\partial c$ vs (wavelength)$^{-2}$ obeyed the linear relation as $\partial n/\partial c = 0.135 + 1.09 \times 10^4$ (wavelength/nm)$^{-2}$ cm^3 g^{-1}. Therefore, the value of $\partial n/\partial c$ at 675 nm was estimated to be 0.159 cm^3 g^{-1}.

The partial specific volume $\bar{\nu}$ of PH3MPS in isooctane at 25 °C was determined to be 1.11_3 cm^3 g^{-1}, using an Anton Paar DMA 5000 density meter. The molecular weight dependence of $\bar{\nu}$ was not detected.

Light Scattering. Scattering intensities were measured for eight samples (F12, F22, ..., F72, and O1) in isooctane at 25 °C on a DAWN DSP light scattering instrument with a flow cell in an angular range from 31° to 148°, using vertically oriented polarized incident light of 633 nm wavelength (He−Ne laser). The reduced scattering intensity R_θ at scattering angle θ was determined as follows.

R_θ was calculated from the detector voltages for the solution V_θ and the solvent $V_{\theta,S}$ using

$$R_\theta = \Phi_\theta n_0 f(n_0)(V_\theta - V_{\theta,S}) \tag{7}$$

where Φ_θ is the instrument constant at angle θ, n_0 is the refractive index of solvent, and $f(n_0)$, which is described in the manual of this instrument, is a known function of n_0; we note that the values of $f(n_0)$ differ little (less that 0.3%) between toluene and isooctane. Φ_{90} (Φ_θ at 90°) was determined from the measured voltage $V_{t,90}$ for toluene at 25 °C and $\theta = 90°$ by use of the equation

$$\Phi_{90} = \frac{R_t}{f(n_0)(V_{t,90} - V_{dark,90})} \tag{8}$$

with R_t (the Rayleigh ratio of toluene) taken as 1.406×10^{-5} cm^{-1} ($V_{dark,90}$ denotes the dark offset voltage obtained with the laser turned off).

Φ_θ other than 90° should not be determined with the same method for Φ_{90} because each detector set except 90° has its own geometrical factors. Therefore, we measured scattering intensities of oligostyrene solutions, whose M_w are 3.44×10^3 or 1.53×10^3, dissolved into toluene ($n_0 = 1.495$), cyclohexane (1.425), or acetone (1.357), and determined Φ_θ by use of the equation

$$\Phi_\theta = N_\theta\Phi_{90} \tag{9}$$

where

$$N_\theta = \frac{V_{90} - V_{90,s}}{V_\theta - V_{\theta,s}} \tag{10}$$

The values of N_θ were almost independent of M_w of used samples and measured concentrations (less than 5 wt %) but dependent slightly on the refractive indices of solvents; in practice, the difference in N_θ's between cyclohexane and acetone is less than 3%. Therefore, the values of N_θ for isooctane ($n_0 = 1.392$) were determined from interpolation of the plots of N_θ vs n_0.

Polymer solutions and the solvent were made optically clean by centrifugation at about 3.2×10^3 times the acceleration of the gravity for 30 min. Each of them was transferred directly

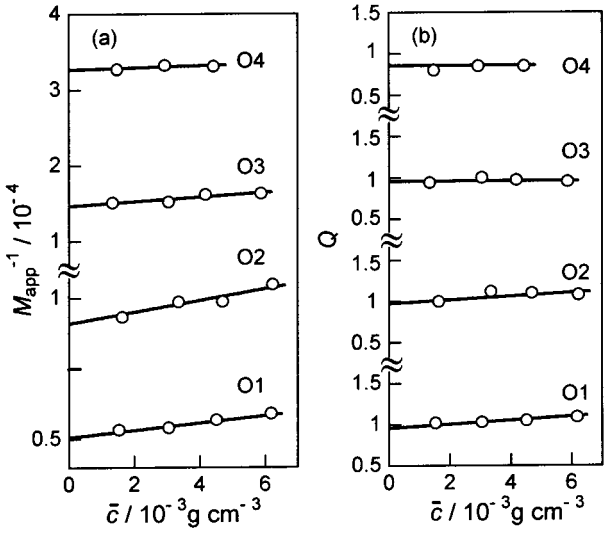

Figure 2. Plots of M_{app}^{-1} vs $\bar{c}$ (a) and Q vs $\bar{c}$ (b) for the indicated PH3MPS samples in isooctane at 25 °C.

into the flow cell with a thin tube (0.5 mm i.d.) which is connected to the flow cell. We made certain with UV absorption that the concentrations of solutions did not change during the measurements described above. To evaluate the reliability of our experimental method, a light scattering measurement in the way described above was also made for the polymacromonomer sample F15-5 in toluene at 25 °C studied before.[22] The M_w value of this sample was determined to be 8.54×10^5. This value is almost equal to 8.22×10^5 measured by the established method in our previous paper.[22]

Viscometry. Viscosity measurements in isooctane at −15, 5, 25, and 45 °C were made using a four-bulb low-shear capillary viscometer of the Ubbelohde type for the sample F12 and a conventional capillary viscometer for the rest; shear-rate effects on the intrinsic viscosity $[\eta]$ were small (less than 1%) when the $[\eta]$ values for this sample from the two types of viscometer were compared. The measurements for the other samples in isooctane at −27 (F22 and F52), −15, 5, 25, and 45 °C were made using the conventional viscometer. Samples O3 and O4 were not studied because the quantity required for viscometry were not obtained.

We measured intrinsic viscosity in the other solvents to investigate solvent effects as described below. First, viscosity measurements for the samples F43 and F61 in isooctane were made to determine $[\eta]$ and viscosity-average molecular weight M_v. Next, we determined $[\eta]$ for the sample F43 in *n*-hexane and in methylcyclohexane at 25 °C.

In all measurements, the flow time was determined to a precision of 0.1 s with the difference between the solvent and solution flow times kept larger than 7 s. The relative viscosity was evaluated by taking account of the difference between the solution and solvent densities. The Huggins plot, the Fuoss−Mead plot, and the Billmeyer plot were combined to determine $[\eta]$ and the Huggins constant k'.

Results

Molecular Weight, Second Virial Coefficient, and Radius of Gyration. Figure 2 illustrates plots of M_{app}^{-1} vs $\bar{c}$ (a) and Q vs $\bar{c}$ (b) constructed from sedimentation equilibrium data. The straight lines in Figure 2b have been drawn with the aid of A_2M_w values evaluated from the plots in Figure 2a. Figure 3 shows the light scattering envelopes for the sample F12, where K is the optical constant; in either figures linear relations are observed facilitating extrapolation to zero angle or zero concentration. This sample has the highest molecular weight studied in this work. The values of M_w, A_2, and the *z*-average radius of gyration $\langle S^2\rangle_z$ obtained are

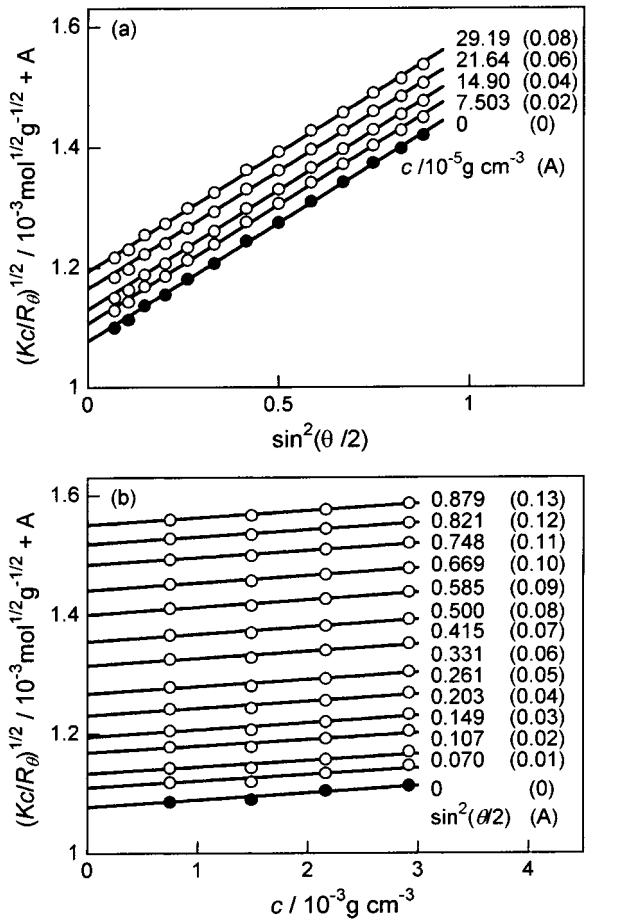

Figure 3. Plots of $(Kc/R_\theta)^{1/2}$ vs $\sin^2(\theta/2)$ at indicated c (a) and $(Kc/R_\theta)^{1/2}$ vs c at fixed scattering angles (b) for sample F12 in isooctane at 25 °C. For clarity, the ordinate values of $(Kc/R_\theta)^{1/2}$ are shifted by A.

Table 1. Results from Light Scattering and Sedimentation Equilibrium Measurements on PH3MPS Samples in Isooctane at 25 °C

sample	$M_w/10^4$	10^4A_2/ cm^3 mol g^{-2}	$\langle S^2\rangle_z^{1/2}$/nm	M_w/M_n[a]	M_z/M_w
		Light Scattering			
F12	87.3	1.5	53.2		
F22	67.4	1.6	44.3	1.13	1.12[a]
F32	51.0	2.0	36.1	1.11	1.10[a]
F42	25.5	2.7	24.5	1.10	1.09[a]
F52	12.6	3.4	15.9	1.10	1.08[a]
F62	6.60	3.9		1.07	1.07[a]
F72	3.67	3.6			
O1	2.09	5.0			
		Sedimentation Equilibrium			
O1	1.98	6			1.0_5[b]
O2	1.10	10 ± 2			1.0_3[b]
O3	0.685	7 ± 2			1.0_5[b]
O4	0.307	7 ± 3			1.1_7[b]

[a] From GPC. [b] From sedimentation equilibrium.

summarized in Table 1, along with those of M_w, A_2, and M_z/M_w from sedimentation equilibrium and M_w/M_n and M_z/M_w from GPC for samples F22, F32, ..., F62. We have not determined these values from GPC for samples F12, F72, O1, O2, O3, and O4, because the extinction coefficients for samples O1, O2, O3, and O4 in isooctane are not independent of molecular weight, whereas the samples F12 and F72 are both at the ends of the calibration curve. The M_w/M_n and M_z/M_w values indicate that our samples are quite narrow in molecular weight

Table 2. Results of Viscometry on PH3MPS Samples in Isooctane at Various Temperatures

		at −27 °C		at −15 °C		at 5 °C		at 25 °C		at 45 °C	
sample	$M_w/10^4$	$[\eta]^a$	k'	$[\eta]^a$	k'	$[\eta]^a$	k'	$[\eta]^a$	k'	$[\eta]^a$	k'
F12	87.3			6.02	0.40	4.20	0.45	3.30	0.40	2.82	0.47
F22	67.4	6.31	0.40	5.15	0.44	3.63	0.40	2.85	0.45	2.46	0.43
F32	51.0			4.08	0.40	2.85	0.39	2.30	0.37	1.95	0.41
F42	25.5			2.23	0.38	1.60	0.39	1.30	0.38	1.10	0.44
F52	12.6	1.45	0.35	1.21	0.35	0.899	0.40	0.753	0.37	0.648	0.42
F62	6.60			0.630	0.37	0.500	0.38	0.432	0.35	0.381	0.38
F72	3.67			0.323	0.4_2	0.275	0.4_0	0.245	0.4_1	0.223	0.4_1
O1	2.04^b			0.179	0.4_2	0.162	0.4_5	0.144	0.4_2	0.137	0.4_2
O2	1.10			0.101	0.5_2	0.0902	0.5_3	0.0859	0.5_6	0.0792	0.5_4

[a] In units of 10^2 cm^3 g^{-1}. [b] The average from light scattering and sedimentation equilibrium.

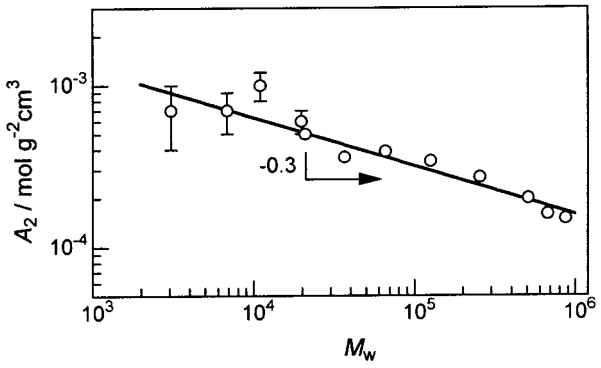

Figure 4. Molecular weight dependence of A_2 for PH3MPS in isooctane at 25 °C.

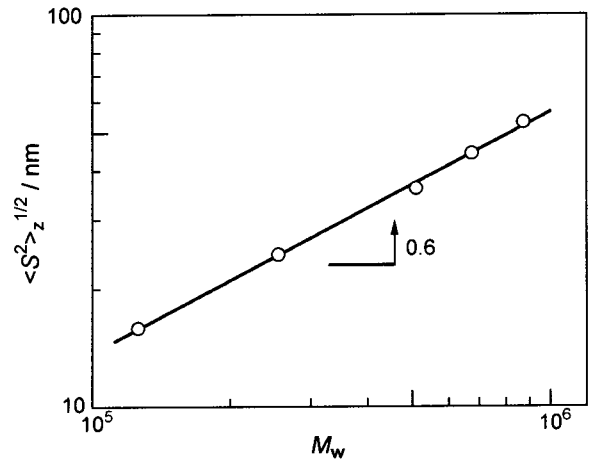

Figure 5. Molecular weight dependence of $\langle S^2\rangle_z^{1/2}$ for PH3MPS in isooctane at 25 °C.

distribution. The M_w value for sample O1 from light scattering agrees (less than ±3%) with that from sedimentation equilibrium.

Figure 4 shows the molecular weight dependence of A_2 for PH3MPS in isooctane at 25 °C. The values A_2 are all of the order 10^{-4} mol cm^3 g^{-2}, and the straight line drawn has a usual negative slope of −0.3 in the molecular weight range studied.

Figure 5 shows the molecular weight dependence of $\langle S^2\rangle_z$ for PH3MPS in isooctane at 25 °C. The data points are fitted by a straight line whose slope is 0.6. This exponent is expected for long flexible chains in good solvents.

Intrinsic Viscosity. The values of $[\eta]$ and Huggins constant k' obtained for PH3MPS samples in isooctane at −27, −15, 5, 25, and 45 °C are summarized in Table 2, along with those of M_w; note that the M_w for O1 is the mean of the value from the two measurements. The

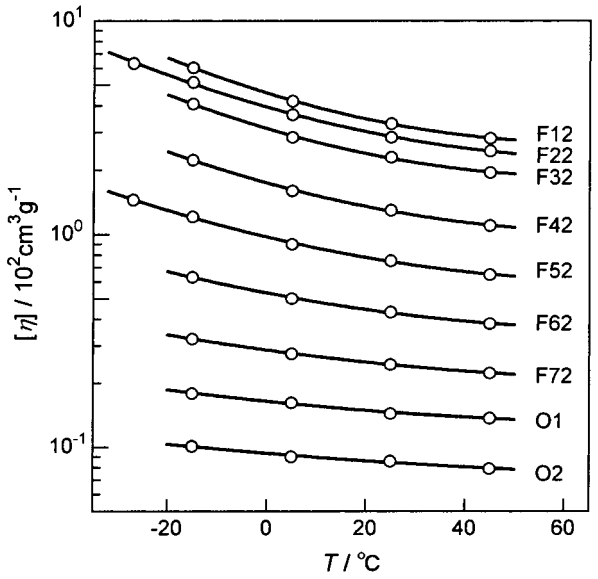

Figure 6. Temperature dependence of $[\eta]$ for the indicated PH3MPS samples in isooctane.

temperature dependence of $[\eta]$ for PH3MPS in isooctane is illustrated in Figure 6. As shown in this figure and Table 2, the value of $[\eta]$ increases with lowering temperature. In fact, the values of $[\eta]$ at −15 °C are 2.1 times as larger as that at 45 °C in the molecular weight range of $M_w > 3 \times 10^5$.

The molecular weight dependence of $[\eta]$ at different temperatures is illustrated in Figure 7. The curve fitting the data points at −15 °C has an inflection point at $M_w \sim 5 \times 10^4$. Its slope is about 1.03 at this point and decreases to about 0.80 for M_w larger than 3×10^5. Below the inflection point, the slope increases gradually with decreasing M_w. The data other than −15 °C show similar M_w dependence, but the slopes of the curve for 45 °C are smaller than those for −15 °C at the corresponding M_w, i.e., 0.85 for $M_w \sim 5 \times 10^4$ and 0.75 for $M_w > 3 \times 10^5$.

Results from viscometry for the sample F43 and F61 are summarized in Table 3. We note that the values of M_v were determined from the solid line for the data at 25 °C in Figure 7. In *n*-hexane at 25 °C, the $[\eta]$ value is 5% larger than that in isooctane at the same temperature, and the $[\eta]$ value in methylcyclohexane at 25 °C is 2% smaller than that in isooctane at the same temperature. The difference in $[\eta]$ among these solvents is only marginal.

Discussion

Data Analysis of Intrinsic Viscosity. The $[\eta]$ of a wormlike chain in the unperturbed state is determined

Table 3. Results of Viscometry on PH3MPS Samples in Different Solvents at 25 °C

	in isooctane			in *n*-hexane		in methylcyclohexane	
sample	$[\eta]^a$	k'	$M_v/10^4$	$[\eta]^a$	k'	$[\eta]^a$	k'
F43	0.665	0.40	10.7	0.695	0.47		
F61	0.603	0.41	9.6			0.593	0.41

[a] In units of 10^2 cm^3 g^{-1}.

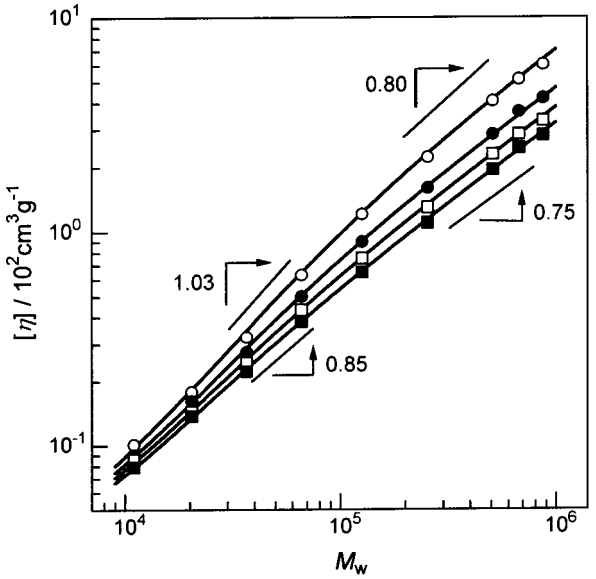

Figure 7. Molecular weight dependence of $[\eta]$ for PH3MPS in isooctane at −15 °C (unfilled circles), 5 °C (filled circles), 25 °C (unfilled squares), and 45 °C (filled squares).

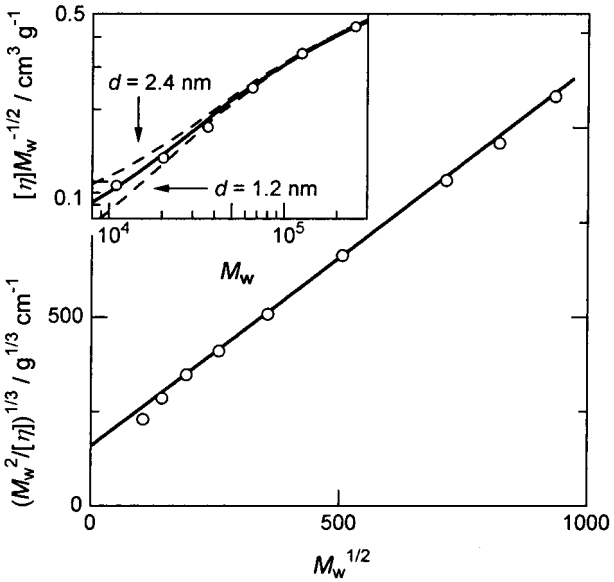

Figure 8. Plot of $(M_w^2/[\eta])^{1/3}$ vs $M_w^{1/2}$ constructed from the data for PH3MPS in isooctane at −15 °C. The solid line in the inset, the theoretical values calculated from Yamakawa−Fujii−Yoshizaki theory for the unperturbed wormlike chain with $q = 11.7$ nm, $M_L = 1000$ nm^{-1}, and $d = 1.8$ nm, and the two dashed lines represent those for $d = 1.2$ nm ($q = 11.4$ nm, $M_L = 930$ nm^{-1}) and $d = 2.4$ nm ($q = 12.3$ nm, and $M_L = 1070$ nm^{-1}).

by L (the contour length), q, and d (the chain diameter).[15,20,21] The first parameter is related to the molecular weight M by

$$L = M/M_L \tag{11}$$

with M_L the molar mass per unit contour length of the chain. Assuming the PH3MPS chain is modeled by the wormlike chain, we first analyze the measured $[\eta]$ in isooctane by a conventional method applicable to typical stiff chain, using the data at low temperature where intramolecular excluded-volume effects would be negligible or small.

1. Conventional Method. According to Bushin et al.[23] and Bohdanecký,[24] the Yamakawa−Fujii−Yoshizaki theory for the intrinsic viscosity $[\eta]_0$ of an unperturbed wormlike cylinder can be expressed in a good approximation as

$$(M^2/[\eta]_0)^{1/3} = I + SM^{1/2} \tag{12}$$

where

$$I = 1.516 \times 10^{-8} I_0 M_L \ (\mathrm{g}^{1/3}\ \mathrm{cm}^{-1}) \tag{13}$$

$$S = 1.516 \times 10^{-8} S_0 (M_L/2q)^{1/2} \ (\mathrm{g}^{1/3}\ \mathrm{cm}^{-1}) \tag{14}$$

with I_0 and S_0 being known functions of $d/2q$. Equation 12 is applicable to a range of $L/2q$ from 3.2 to 2000 for weakly stiff chains ($d/2q \sim 0.1$) and from 0.4 to 300 for typical stiff chains ($d/2q \sim 0.01$).[24] In such a range of chain length, the Bushin−Bohdanecký plot of $(M_w^2/[\eta])^{1/3}$ vs $M_w^{1/2}$ should give a straight line whose intercept and slope equal I and S, respectively.

Figure 8 shows the Bushin−Bohdanecký plot constructed from the present data in isooctane at −15 °C. The plotted points follow the straight line except the data point for O2, yielding the two values $I = 158$ g$^{1/3}$ cm^{-1} and $S = 1.00$ g$^{1/3}$ cm^{-1}. The downward deviation from the line for $M_w^{1/2}$ below 150 can be ascribed to the inapplicability of eq 12 to short chains, but it may be utilized for finding one more relation and hence for uniquely determining the three parameters, q, M_L, and d. The procedure is as follows.

First, different sets of q, M_L, and d are evaluated from the above I and S values and appropriately chosen d values. Then the $[\eta]$ values computed from the Yamakawa−Fujii−Yoshizaki theory[15,20,21] with those parameter sets are compared with the experimental data. The solid curve in the inset of Figure 8 represents the theoretical values for $d = 1.8$ nm ($q = 11.9$ nm and $M_L = 1010$ nm^{-1}), while the dashed curves represent those for $d = 1.2$ nm ($q = 11.4$ nm and $M_L = 930$ nm^{-1}) and $d = 2.4$ nm ($q = 12.3$ nm and $M_L = 1070$ nm^{-1}). It can be seen that the d value of 1.8 nm (with $q = 11.9$ nm and $M_L = 1010$ nm^{-1}) gives the best fit to the data points.

The M_L value of 1010 nm^{-1} estimated above (for PH3MPS in isooctane at −15 °C) is consistent with the chemical structure of PH3MPS if we assume that the conformation of main chain is the 7_3 helix, i.e., $M_L = 1005$ nm^{-1}; note that this value was calculated from the pitch per monomeric unit of the helix (0.197 nm).[25] The q value at −27 °C was estimated at 15.4 nm when M_L and d were assumed to be the same as those at −15 °C.

Table 4. Molecular Parameters for PH3MPS in Isooctane at Various Temperatures

T/°C	$M_L/10^3$ nm^{-1}	d/nm	q/nm	B/nm
−27	1.01[a]	1.8[a]	15.4	(1.7)
−15	1.01	1.8	11.9	(1.7)
5	1.01[a]	1.8	7.7	1.7
25	1.01[a]	1.8	6.1	1.7
45	1.01[a]	1.8	5.0	1.7

[a] Assumed.

The $[\eta]$ data at higher temperatures were difficult to determine by the same method because the Bushin−Bohdanecký plots[23,24] do not obey the linear relation in the M_w range. This is due to the excluded-volume effect being much more significant than that at −15 °C. Therefore, the $[\eta]$ data are analyzed on the basis of the wormlike chain model with excluded-volume effect in the next section.

2. Consideration of Excluded-Volume Effect. As shown in the previous section, the excluded-volume effects on $[\eta]$ are not negligible at the temperatures higher than −15 °C. In the following, we analyze $[\eta]$ data with the aid of the quasi-two-parameter (QTP) theory[15,26,27] for wormlike or helical wormlike bead chains. This theory allows an accurate description of $[\eta]$ for linear flexible and semiflexible polymers over a broad range of molecular weight.[15,28] The viscosity−radius expansion factor α_η [$=([\eta]/[\eta]_0)^{1/3}$] in the QTP scheme is expressed by

$$\alpha_\eta^{\,3} = (1 + 3.8\tilde{z} + 1.9\tilde{z}^2)^{0.3} \tag{15}$$

if the Barrett function is adopted.[29] Here, $\tilde{z}$ is the scaled excluded-volume parameter defined by

$$\tilde{z} = \frac{3}{4}K(N)\left(\frac{3}{2\pi}\right)^{3/2}\frac{B}{2q}N^{1/2} \tag{16}$$

where N is the Kuhn statistical segment number defined by $N = L/2q$, $K(N)$ is a known function of N (cf. eq 8.46 in ref 21 or eq 50 in ref 27), and B is the excluded-volume strength with the unit of length.

Equations 15 and 16 indicate that B needs to be known (in addition to q and M_L) in order to evaluate theoretical α_η^3. A curve-fitting procedure was employed for the determination of the parameters, but M_L at any temperature was assumed to be the same as that at −15 °C; we note that the three parameters (d, q, and B) can uniquely be determined from the $[\eta]$ data when the value of M_L is fixed. The parameters obtained are summarized in Table 4 with those at −15 °C. It is reasonable to take the B value at −15 °C to be 1.7 nm because the values estimated at other temperatures are invariably 1.7 nm.

Figure 9 compares the experimental $[\eta]M_w^{-1/2}$ for PH3MPS in isooctane at indicated temperatures with the theoretical solid lines calculated with the parameters in Table 4. The agreement is satisfactory at all the temperatures. The dashed line at each temperature refers to the unperturbed state (i.e., $B = 0$). The excluded-volume effect is almost invisible at −15 °C but becomes appreciable with increasing temperature. In particular, it is significant for $M_w > 10^5$ at 45 °C. Thus, we conclude that the excluded-volume effect becomes visible as the temperature is raised not because of the excluded-volume interactions (B) but due to the increasing flexibility.

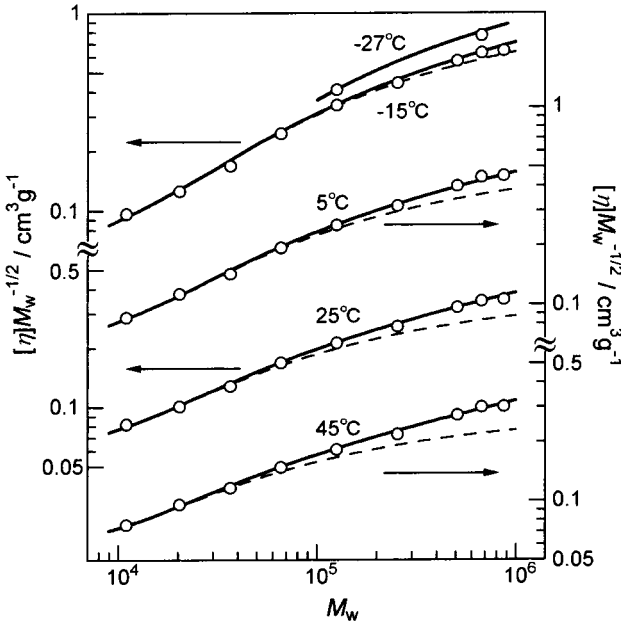

Figure 9. Comparison between the measured $[\eta]M_w^{-1/2}$ for PH3MPS in isooctane at indicated temperatures and the theoretical values (solid lines) calculated with the parameters in Table 4. Dashed lines represent theoretical values for $B = 0$.

Data Analysis of Radii of Gyration. As shown above, excluded-volume effects on $[\eta]$ for PH3MPS in isooctane at 25 °C are significant at high M_w and explained quantitatively by the QTP theory. Within the framework of this theory, the radius expansion factor α_s [$\equiv(\langle S^2\rangle/\langle S^2\rangle_0)^{1/2}$] is a universal function of $\tilde{z}$, where $\langle S^2\rangle_0$ denotes the unperturbed mean-square radius of gyration and is given by[30]

$$\langle S^2\rangle_0 = (2q)^2\left[\frac{1}{6}N - \frac{1}{4} + \frac{1}{4N} - \frac{1}{8N^2}(1 - e^{-2N})\right] \tag{17}$$

for the wormlike chain. Adopting the Domb−Barrett equation[31] for α_s^2, we have

$$\alpha_s^{\,2} = \left[1 + 10\tilde{z} + \left(\frac{70\pi}{9} + \frac{10}{3}\right)\tilde{z}^2 + 8\pi^{3/2}\tilde{z}^3\right]^{2/15}[0.933 + 0.067\exp(-0.85\tilde{z} - 1.39\tilde{z}^2)] \tag{18}$$

Equation 18 is known to accurately describe experimental data for flexible and semiflexible polymers over a broad range of molecular weight.[15,28]

Equations 17 and 18 indicate that $\langle S^2\rangle$ in the perturbed state is characterized by three parameters: M_L, q, and B. A curve-fitting procedure was employed for our analysis with q assumed to the values determined from $[\eta]$ (q = 6.1 nm); we note that M_L and B can uniquely be determined from the present $\langle S^2\rangle_z$ data when the value of q is fixed. The parameters were estimated to 900 nm^{-1} for M_L and 1.7 nm for B, respectively. Figure 10 shows that the theoretical solid curve calculated with these parameters closely fits the data points over the whole range studied.

As is known, the analysis of $\langle S^2\rangle_z$ for polydisperse samples by eq 17 gives a value of M_L that is smaller than the true value. If $N > 5$, this polydispersity effect may be corrected by multiplying M_L by M_z/M_w. In fact, the M_L value from $\langle S^2\rangle_z$ is about 0.89 times as large as that from $[\eta]$. On the other hand, GPC measurements

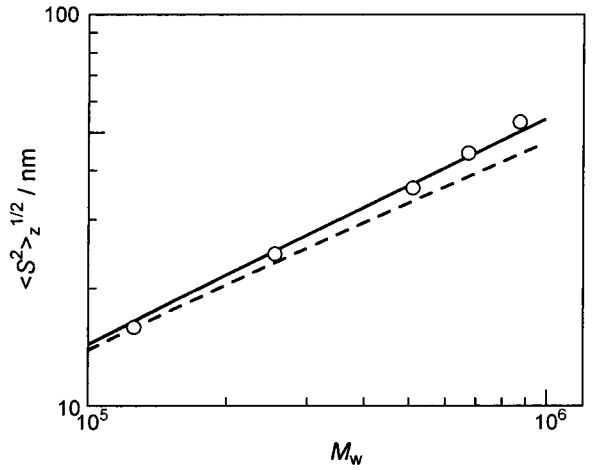

Figure 10. Comparison between the measured $\langle S^2\rangle_z^{1/2}$ for the PH3MPS in isooctane at 25 °C and the theoretical solid curve for the perturbed wormlike chains with the parameters M_L = 900 nm^{-1}, q = 6.1 nm, and B = 1.7 nm. The dashed line represents theoretical values for $B = 0$.

and sedimentation equilibrium gave a value around 1.1 for M_z/M_w of our PH3MPS samples. Thus, we find that the $[\eta]$ and $\langle S^2\rangle_z$ data are explained consistently with the parameters described above, which in turn shows that the assumption for M_L is correct.

Conclusions

We have determined intrinsic viscosity $[\eta]$, z-average mean-square radius of gyration $\langle S^2\rangle_z$, and A_2 as functions of weight-average molecular weight M_w for poly{*n*-hexyl-[(*S*)-3-methylpentyl]silylene} (PH3MPS) in isooctane, *n*-hexane, and methylcyclohexane at different temperatures. The following conclusions have been drawn from the analysis of $[\eta]$ and $\langle S^2\rangle_z$ data on the wormlike chain with excluded volume.

1. The molar mass per unit contour length 1.01×10^3 nm^{-1} for the PH3MPS in isooctane is consistent with the value calculated for the model of 7_3 helix.

2. In isooctane, the persistence length q remarkably increases from 5.0 nm at 45 °C to 15.4 nm at −27 °C with decreasing temperature.

3. The $[\eta]$ values in *n*-hexane and methylcyclohexane were substantially equal to that in isooctane at the same temperature. This finding suggests that the persistence lengths of PH3MPS are not affected by small difference of the shape of solvent molecules.

Acknowledgment. The authors gratefully acknowledge Kei-ichi Torimitsu and Hideaki Takayanagi for their support. A.T. thanks Yamashita Sekkei Ltd. for the chair professorship.

References and Notes

(1) West, R. *J. Organomet. Chem.* **1986**, *300*, 327−346.
(2) Miller, R. D.; Michl, J. *Chem. Rev.* **1989**, *89*, 1359−1410.
(3) Michl, J.; West, R. Electronic Structure and Spectroscopy of Polysilylenes. In *Silicon-Based Polymers*; Chojnowski, J., Jones, R. G., Ando, W., Eds.; Kluwer: Dordrecht, 2000.
(4) Fujiki, M. *J. Am. Chem. Soc.* **1994**, *116*, 6017−6018.
(5) Fujiki, M. *J. Am. Chem. Soc.* **1994**, *116*, 11976−11981.
(6) Fujiki, M. *Appl. Phys. Lett.* **1994**, *65*, 3251−3253.
(7) Fujiki, M. *J. Am. Chem. Soc.* **1996**, *118*, 7424−7425.
(8) Yuan, C.-H.; Hoshino, S.; Toyoda, S.; Suzuki, H.; Fujiki, M.; Matsumoto, N. *Appl. Phys. Lett.* **1997**, *71*, 3326−3328.
(9) Fujiki, M.; Toyoda, S.; Yuan, C.-H.; Takigawa, H. *Chirality* **1998**, *10*, 667−675.
(10) Ichikawa, T.; Yamada, Y.; Kumagai, J.; Fujiki, M. *Chem. Phys. Lett.* **1999**, *306*, 275−279.
(11) Toyoda, S.; Fujiki, M. *Chem. Lett.* **1999**, 699−700.
(12) Koe, J. R.; Fujiki, M.; Nakashima, H. *J. Am. Chem. Soc.* **1999**, *121*, 9734−9735.
(13) Koe, J. R.; Fujiki, M.; Motonaga, M.; Nakashima, H. *Chem. Commun.* **2000**, 389−390.
(14) Fujiki, M. *J. Am. Chem. Soc.* **2000**, *122*, 3336−3343.
(15) Yamakawa, H. *Helical Wormlike Chains in Polymer Solutions*; Springer: Berlin, 1997.
(16) Norisuye, T. *Prog. Polym. Sci.* **1993**, *18*, 543−584.
(17) Kratky, O.; Porod, G. *Recl. Trav. Chim.* **1949**, *68*, 1106.
(18) Cotts, P. M. *Macromolecules* **1994**, *27*, 2899−2903.
(19) Terao, K.; Terao, Y.; Teramoto, A.; Nakamura, N.; Terakawa, I.; Sato, T.; Fujiki, M. *Macromolecules* **2001**, *34*, 2682−2685.
(20) Yamakawa, H.; Fujii, M. *Macromolecules* **1974**, *7*, 128−135.
(21) Yamakawa, H.; Yoshizaki, T. *Macromolecules* **1980**, *13*, 633−643.
(22) Terao, K.; Nakamura, Y.; Norisuye, T. *Macromolecules* **1999**, *32*, 711−716.
(23) Bushin, S. V.; Tsvetkov, V. N.; Lysenko, E. B.; Emelyanov, V. N. *Vyskomol. Soedin., Ser. A* **1981**, *A23*, 2494.
(24) Bohdanecký, M. *Macromolecules* **1983**, *16*, 1483−1492.
(25) Miller, R. D.; Farmer, B. L.; Fleming, W.; Sooriyakumaran, R.; Rabolt, J. *J. Am. Chem. Soc.* **1987**, *109*, 2509−2510.
(26) Yamakawa, H.; Stockmayer, W. H. *J. Chem. Phys.* **1972**, *57*, 2843−2854.
(27) Shimada, J.; Yamakawa, H. *J. Chem. Phys.* **1986**, *85*, 591−600.
(28) Norisuye, T.; Tsuboi, A.; Teramoto, A. *Polym. J.* **1996**, *28*, 357−361.
(29) Barrett, A. J. *Macromolecules* **1984**, *17*, 1566−1572.
(30) Benoit, H.; Doty, P. *J. Phys. Chem.* **1953**, *57*, 958.
(31) Domb, C.; Barrett, A. J. *Polymer* **1976**, *17*, 179.

MA010212W